Hindawi
Wireless Communications and Mobile Computing
Volume 2022, Article ID 3525197, 11 pages
https://doi.org/10.1155/2022/3525197

Research Article

Optimal Recognition of Volleyball Player's Arm Movement Track Based on Embedded Microprocessor

Ming Liu,[1] **Jingtao Wu**,[2] **and Jiangang Tao**[3]

[1]*Department of Public Physical Art Education, Zhejiang University, Hangzhou, 310058 Zhejiang, China*
[2]*College of Physical Education, Leshan Normal University, Leshan, 614000 Sichuan, China*
[3]*College of Marxism & Mental Health Education Center, Yanshan University, Qinhuangdao 066004, China*

Correspondence should be addressed to Ming Liu; michael616504@zju.edu.cn

Received 25 December 2021; Revised 26 January 2022; Accepted 23 February 2022; Published 13 April 2022

Academic Editor: Shalli Rani

An embedded microprocessor is the core part of the integrated circuit system, and it represents one of the highest levels of a digital integrated circuit design. Therefore, the design of low-power embedded microprocessors has become an important research direction in the integrated circuit design. Volleyball has always been a very important sport in our country, and it is a sport that the masses of people like to see. The basic techniques of volleyball include ready posture and movement, serving, hot ball, passing, smashing, and netting. The research content of this article is a simulation study of volleyball players' arm trajectory optimization recognition. In response to the above problems, this paper proposes an optimized recognition method based on the volleyball player's arm motion trajectory. The simulation results show that the method has high recognition accuracy and provides a strong scientific basis for improving the volleyball players' spike skills. Without interference from the right arm, the controller input and position tracking error will not fluctuate in $1 \le T \le 3$, the controller input is stable, and the output error is zero. Based on the above simulation analysis, it can be seen that the control method does not require the robot kinematics and dynamics model to generate any regression matrix when designing the controller. The controller is suitable for the performance tracking of humanoid robot arms.

1. Introduction

The anthropomorphic double-arm robot has its unique advantages in industrial fields such as precision grinding, precision assembly, and heavy load handling. It is the direction of the intelligent development of the next generation of industrial robot arms. At the same time, volleyball, as the only collective sports event to win the Olympic championship in China's three major balls, occupies a very important position in the hearts of Chinese people. The Chinese women's volleyball team won the 2019 Women's Volleyball World Cup and successfully defended the title. This is the tenth World Championship won by the Chinese women's volleyball team, and it is also a special birthday gift they sent to the 70th birthday of the People's Republic of China. General Secretary Xi Jinping called to congratulate everyone and encouraged everyone to continue to maintain high fighting spirit, not be arrogant or impetuous, and achieve better results. The spirit of women's volleyball encourages all walks of life to struggle forward. As the development of the world volleyball team enters the new century, volleyball has also developed rapidly. In recent years, international competitions have continued to increase. Various countries are also actively participating in preparations, whether in the overall team tactics or player physical fitness. Quickly, in addition, it has attracted a large number of commercial resources, and the commercial development of volleyball has also become colorful, so this has increased the healthy competition between sports teams in various countries, thereby greatly promotes the popularity of volleyball worldwide, and also makes volleyball more professional and commercial.

From the evolution of apes to humans, human use of various tools is becoming more flexible and even making complex arm movements, which is more challenging for the analysis of athlete arm trajectories. More and more arm movement makes human upper limbs, especially the

arms and fingers, not only developed but also very flexible, as if they were skillful [1, 2]. The flexibility of the joints tends to be perfect, the structural characteristics are very reasonable, the movement can be optimized and the most flexible, and the ability to adapt to the environment is extremely strong, which makes the human survival ability easier than other organisms [3, 4]. From ancient times to the present day, human beings have been learning and exploring the world from the rich world. Many of the inspirations for human technologies and inventions come from the colorful natural world [5, 6]. Therefore, the natural world is the source of human progress and development and an inexhaustible treasure trove of ideas and inventions [7, 8]. Learning from nature, imitating various movements of creatures to serve humanity has developed into a discipline, i.e., bionics [8, 9]. As the most important branch of research in bionics, the research of humanoid itself is also one of the most popular research fields at present [10, 11]. In recent years, there have been many studies at home and abroad where two single-arm robots coordinate and cooperate with each other to accomplish a certain task and have achieved many research results [12, 13]. However, it is difficult to deal with emergency accidents by a simple combination of two one-handed robots to complete complex and flexible actions like humans [14, 15]. Therefore, it is very meaningful to study and implement the dual-arm robot to flexibly and steadily perform various actions like humans in a complex environment [16, 17]. The traditional robot trajectory construction method relies on manual programming by the operator, and the efficiency is relatively low [18, 19]. In recent years, a method based on imitation-based automatic generation of robot trajectories has received increasing attention from researchers [5, 20]. This method has higher efficiency than traditional methods and has the advantages of strong adaptability for different execution tasks [21, 22]. It enables robots to learn new skills and knowledge by interacting with other individuals in the environment, such as humans or other robots, just like humans [8]. The automatic generation method of movement track based on imitation makes the robot more adaptable. By observing the movement of the teacher with marked points, the movement information of the teacher can be quickly and accurately obtained, and the computer passes the obtained data through. A certain algorithm is processed to generate a reasonable robot trajectory and store it and then controls the robot to repeat the same actions as the teacher, so that the robot learns useful actions and enables it to quickly adapt to new tasks and environments [23, 24].

Learning the spatiotemporal representation of motion information is essential for human action recognition. However, most existing features or descriptors cannot effectively capture motion information, especially for long-term motion. To solve this problem, Shi et al. proposed a long-term motion descriptor called a sequential depth trajectory descriptor (sDTD). Specifically, Shi et al. project dense trajectories into a two-dimensional plane and then uses CNN-RNN networks to learn effective representations of long-term motion. Unlike the popular two-stream ConvNets, the sDTD stream is introduced into a three-stream framework in order to recognize actions from video sequences. Therefore, this three-stream framework can simultaneously capture the static spatial features, short-term motion and long-term motion in the video. Extensive experiments were performed on three challenging data sets: KTH, HMDB51, and UCF101. Experimental results show that Shi et al.'s method has the most advanced performance on the KTH and UCF101 datasets and is comparable to the latest method on the HMDB51 dataset [25]. Fahn et al. introduced a gesture recognition method for human-machine interface. This recognition method is based on a learning ranking model. Experimental results show that the AdaRank model is effective for improving recognition accuracy. Combining the learning ranking model with the hand movement trajectory has made a breakthrough in modeling a complex combination of 8 recognized gestures. The construction of the gesture recognition system can effectively detect the gestures of one hand or two hands in basic directions (such as moving up, moving down, moving left, and moving right). In order to make users more friendly to the proposed system, Fahn et al. can combine basic directions and expand into more gestures for applications. Experimental results show that Fahn et al.'s method has high performance and can run in real time. For practical applications, the accuracy of this method is also very high [26]. The energy expenditure of the human arm is important for seeking the optimal human arm trajectory. Zhou et al. proposed a new method to calculate the metabolic energy expenditure of the human arm movement, aimed at revealing the relationship between the energy expenditure and the arm movement trajectory and the contribution of acceleration and arm direction. Zhou et al. studied the horizontal motion of the human arm with the Qualisys motion capture system, and motion data were postprocessed by biomechanical models to obtain metabolic consumption, including results on arm motor kinematics, kinetics, and metabolic energy expenditure [27].

This study starts from the whole and observes the characteristics of shoulder dysfunction, such as morphology, muscle strength, mobility, proprioception, etc., using the shoulder joint as a ring, and putting it into the whole whip chain from the torso to the arm. For analysis, the simulation test system was applied to volleyball for the first time to test the strength, speed, power, etc. of spiking, and combined with EMG, infrared high-speed camera and other tests, a comprehensive analysis of the dynamic mechanism of shoulder dysfunction. The function of proprioception is to receive external stimuli and structural deformations produced by joint muscle movements and transmit this information to the center to adjust limb position and muscle activity, so as to protect and maintain joint stability and avoid sports injuries caused by excessive movements. This article observes the morphological characteristics of people with shoulder dysfunction; tests their activity, muscle strength, and proprioception; and observes the changes in proprioception after static strength exercise fatigue; through simulation tests, surface electromyography, and biomechanical tests, the analysis caused dysfunction dynamic mechanism. In this paper, the automatic generation method of robot trajectory based on

imitation is to record and process the motion data of the teacher and then map it into the corresponding trajectory of the robot and optimize it to make the robot reproduce the motion of the teacher.

2. Proposed Method

2.1. Volleyball Player Movement Analysis. In volleyball spiking, upper limb movements are all coordinated by shoulder straps, shoulder joints, elbow joints, radial ulnar joints, wrist joints, and finger joints. The movement of the shoulder strap always follows the movement of the shoulder joint to increase the amplitude of the upper arm movement. The swinging action of the swing arm is to lift the shoulder joint as the axis directly to the back of the shoulder and accelerate forward and upward. Therefore, during jumping and air strikes, the movement of the upper limb can be decomposed into a shoulder strap: shoulder blade bony rotation-rotation-down maneuver-forward extension and lowering; shoulder joint motion: upper arm flexes-inner rotation extension when shoulder joint abducts; and elbow joint motion: when swinging the upper arm, the triceps contract explosively to straighten the elbow joint. The flexor muscles of the wrist and fingers contract, and although the force generated by the action is not large, the effective transmission of momentum, the determination of the final position of the end ring, and the decisive influence on the final state. During the whiplash of the upper limbs, the muscles that complete the exercise usually first passively elongate and then contract to apply force. Muscles, a form of work that is forced to rapidly centrifugal contract and then turn into centripetal contraction, is called "stretch-shorten cycle."

2.2. Arm Trajectory Model. The typical joint morphology is mainly on the kinematic joint surface (the articular surface is the contact surface of each related bone that constitutes the joint. Each joint includes at least two articular surfaces, generally one convex and one concave. The convex one is called the joint head, and the concave one is called the joint socket), when it is described in joint kinematics. The shape of the articular surface is mostly a curved surface or a slightly curved surface. This forms a concave-convex relationship at the joint. The concave-convex relationship of the joints allows them to adapt to each other, increase the surface area to dissipate the contact force, and help guide the movement between bones. Almost half of the humeral bone of the shoulder joint is a solid sphere. It forms the convex surface of the glenohumeral joint. In this concave-convex relationship, there are three basic forms of motion: rolling, sliding, and rotating. When the human arm is in motion, three types of motion will move on the convex and concave surfaces. The definitions for scrolling, sliding, and rotating are shown in Table 1.

Since rotation is more important for the humanoid dual-arm robot in the later period, the following introduction and examples are given here. The humanoid dual-arm robot is capable of having a stronger grip and a longer arm span than humans, which mimics the human arm structure to complete a similar movement to the human arm. One of the main ways of bone rotation is through the rotation of its joint surface to counter the articular surface of another bone. Generally, it mainly occurs in the rotation of the forearm and the glenohumeral joint and the flexion and extension of the hip joint.

In the process of arm movement, the shoulder joint, elbow joint, and wrist joint complex mainly rely on the rotation method. In order to better evaluate the movement of the arm, this section uses the triangle rule to study the shoulder joint as an example, as shown in Figure 1. In the triangle, the value of the trigonometric function can be calculated through the relationship between the angle and the edge. The sides of the triangle can represent physical quantities such as distance, force, and speed. Here, we first define the representation of right-angle trigonometric functions in biomechanical relations, sine $\sin(\alpha)$, cosine $\mathrm{Cos}(\alpha)$, tangent $\mathrm{Tan}(\alpha)$, and cotangent $\mathrm{Cot}(\alpha)$, where each trigonometric function represents a specific given angle value. If the vector representing two sides is known in a right triangle, the third side is the hypotenuse, which can be determined by the Pythagorean theorem. If, in addition to a right angle, a side and an angle are known in a right triangle, then the remaining sides of the triangle can be represented by one of four trigonometric functions. The angle can be obtained by knowing any two sides using an inverse trigonometric function. The angle of insertion of the deltoid muscle in the shoulder joint is 45 degrees from the bone. Based on the selected work coordinate reference system, the rectangular part muscle force M is synthesized by Mx parallel to the arm and perpendicular to the arm My.

When the elbow joint is subjected to external resistance, the muscle provides power for the arm to resist the resistance. It belongs to the internal force category of the elbow joint. This muscle strength can be decomposed into Mx parallel to the forearm (radial) and vertical My by the right triangle method. These forces affect the stability of the joint. When the muscle component My parallel to the forearm passes through the axis of rotation at the elbow joint, there is no torque, so there is no rotation. When the component force, my perpendicular to the forearm passes through the rotation axis, a torque is generated, and therefore, rotation occurs. This vertical component also produces a tangential force on the humeral radius joint. The direction is along the positive direction of the Y axis.

Arm movements include plate support, pull-up, push-ups, and back push-ups. Embedded processor is the core of the embedded system, which is the hardware unit of control and auxiliary system operation. As the core of the embedded system, the embedded processor undertakes the important tasks of control and system work, making the host equipment function intelligent, flexible design, and simple operation.

2.3. Principle of Identification. In the process of identifying the trajectory of the volleyball player's arm, we first obtain the joint points of the human arm movement, extract the key feature point trajectory of the arm movement trajectory, obtain the data of the arm trajectory feature point of each frame of image, and obtain the dynamic volleyball player

Table 1: Three kinds of motion definition in joint kinematics.

Exercise method	Definition	Performance of joints in motion
Scroll	Multiple points of one rotating joint surface are in contact with multiple points of another joint surface	Tyre movement on the road
Slide	A single point of one joint surface is in contact with multiple points of another joint surface	Tires slip on smooth ice
Spin	Rotation of a single point on one joint surface with a single point on another joint surface	The ball turns a little on the ground

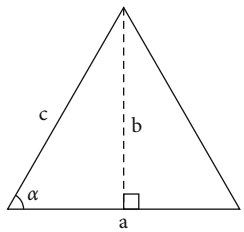

Figure 1: The triangle rule.

arm movement sequence diagram. We establish a volleyball player arm movement trajectory recognition model to complete the volleyball player arm movement trajectory recognition. a represents the distance between the wrist joint and the shoulder joint, b represents the distance between the wrist joint and the elbow joint, and c represents the distance between the elbow joint and the shoulder joint. Then, using Equation (1), we first obtain the coordinates of the human arm joint.

$$\alpha^{\partial}(\Gamma) = \frac{\varphi(\partial) \times X}{c \times M(\alpha) \cdot b} * (Z). \tag{1}$$

In the formula, $M(\alpha)$ represents the distance between the joints of the left arm and the shoulder joints in the space. $\phi(\partial)$ represents the distance between the joints and the shoulder joints. Vector Z represents the change range of joint point of arm movement. Suppose that $\eta(I_d, I_Y)$ represents any pixel in the single-pixel picture of the volleyball player's arm movement in a certain frame, and I_d and I_Y represent the horizontal axis and ordinate $\partial_n(I_d, I_Y)$ of I, respectively, and represent the subsequent n-frame single-pixel athlete's arm movement picture, Equation (2) gets the data of the feature points of the arm's motion trajectory for each frame of the image:

$$\eta(\tau) = \frac{\eta(I_d, I_Y) \otimes \partial_n(I_d, I_Y)}{I_d \otimes I_Y} \times \alpha^{\partial}(\Gamma). \tag{2}$$

Assuming that $I'(I'_x, I'_y)$ represents the corner point of the right arm end and then uses Equation (3) to obtain the data of the arm trajectory feature points of each frame image:

$$I'\left(I'_x, I'_y\right) = \frac{\partial_n(I_d, I_Y) \times \eta(I_d, I_Y)}{I_d \otimes \lambda(M)}. \tag{3}$$

In the formula, $\lambda(M)$ represents the offset of the depth feature from the original position. Assuming that $f_i(I, Y)$ represents the segmentation position feature of the hand region, $B(\mu, \nu)$ represents the processed motion trajectory, and θ represents the conversion data of the lower arm of the arm, and then, we use Equation (4) to obtain the dynamic volleyball player arm motion sequence diagram.

$$\omega_b^{a^n}(\ell, l) = \left[x'_b\right] \otimes \frac{(E \otimes f_i(I, Y)}{B(\mu, \nu)} \times \theta. \tag{4}$$

In the formula, x'_b represents the characteristic parameter of the arm motion, and E represents the characteristic value of the connected area to mark the initial frame image. Based on the above, formula (5) is used to build a volleyball player arm movement trajectory recognition model.

$$\mu(\wp) = \frac{[fi(I, Y)] \oplus \alpha\partial(\Gamma) * (Z)}{\omega_b^{a^n}(\ell, l) \otimes \lambda(\xi)}. \tag{5}$$

In the formula, $\lambda(\xi)$ represents the change range of joint trajectory. The above can explain the principle of volleyball player arm movement trajectory recognition, which can be used to identify the volleyball player arm movement trajectory.

In the process of recognizing the trajectory of the volleyball player's arm movement, the fusion of the background difference principle is first used to detect the athlete's movement trajectory, and the dynamic arm tracking is performed by the particle filter of the color histogram. Suppose that u_t represents the corresponding pixel of the background image, u_{t+1} represents the updated pixel of the volleyball player arm motion background image, and it represents the pixel of the current frame volleyball player arm motion image; then, we use formula (6) to collect the detected volleyball player's arm motion sequence images.

$$\mu_{t+2} = \begin{cases} \mu_t, I_t(x, y), \\ \alpha_{\mu_{t+1}} + (1\text{-}\alpha) I_t \otimes I_f. \end{cases} \tag{6}$$

In the formula, α represents the update rate of the background model, I_f represents the mask value of the pixels of the current frame image. In the RGB recognition of the volleyball player's arm movement trajectory, the skin color of the arm is yellowish, and the brightness of the pixels of the

skin color is greater. The pixel corresponding to the skin color of the volleyball player's arm corresponds to the brightness $\chi(p)$ representing the back projection image of each frame of arm movement, and then, the binary image of the arm movement trajectory is detected by using

$$v\_\text{temp} = \begin{cases} \chi(p) \otimes \eta(\beta), \\ v \times \partial(Y) \times r. \end{cases} \tag{7}$$

In the formula, $\partial(Y)$ represents the different channels of the RGB image, $\eta(\beta)$ represents the proportional coefficient of the skin color of the athlete's arm movement, and r represents the pixels of the skin area of the moving arm. Suppose that $w_k^i(x_{0:k})$ is the weight representing the time of the ith particle $k-1$, w_{k-1}^i is the likelihood probability observed by the volleyball player's arm motion trajectory system, and the weight of the particle is obtained by calculating the Barr coefficient of the color histogram.

In the formula, $P(u)$ represents the color histogram of the arm motion area where each particle is located, and $q(u)$ represents the sensitivity of the color space to light.

In summary, it can be explained that in the process of volleyball player arm movement trajectory recognition, the background difference principle is first used to detect the athlete's movement trajectory, and the color histogram particle filter is used for dynamic arm tracking, which provides a volleyball player arm movement trajectory recognition.

2.4. The Processing Power of the Microprocessor. We know that a program written in a high-level language needs to be compiled, assembled, and linked with a compiler, assembler, and linker, respectively, to generate object codes that can be directly executed by the microprocessor. The object code consists of a series of computer instructions. We define the performance of a microprocessor as

$$\text{PER} = \frac{1}{\text{EXET}}. \tag{8}$$

In the above formula, EXET represents a period of program execution time, and another commonly used performance indicator is MIPS, that is, how many millions of instructions are executed per second

$$\text{MIPS} = \frac{\text{EIC}}{\text{ET}(s) * 10^6}. \tag{9}$$

The total service delay can be expressed as follows:

$$T(\text{TA}) = \left\{ \frac{\text{Task}}{c} + wm, \frac{\text{Task}}{c_2} + wm, \frac{\text{Task}}{c_3} + wm, \cdots, \frac{\text{Task}}{c_m} + wm \right\} + \phi. \tag{10}$$

The solution of the task distribution coefficient can be transformed into a vector solution, which is modeled as the following optimization problem:

$$\begin{aligned} \sum_{i=1}^{k} \text{TA}(i) &= \text{Task}, \\ I = \prod_{i=1} [\text{Task}_{\min}, \text{Task}_{\max}] &= \prod_{i=1} [0, \text{Task}]. \end{aligned} \tag{11}$$

The total service response delay under the condition of no failure can be expressed as follows:

$$t = \max \left\{ \frac{D}{C} + Wl, \frac{D_c}{C_c} + Wl \right\}. \tag{12}$$

The communication delay between computing nodes in the CE-IIoT architecture can be expressed as follows:

$$W = \frac{D}{L} \times \frac{T(1+P)}{1-P}. \tag{13}$$

Then, the time delay for a successful transmission of a data packet is calculated as follows:

$$\begin{aligned} T &= \frac{L}{R}, \\ W_{vi,vj} &= \frac{D}{r} \times \frac{1-l}{1+l}. \end{aligned} \tag{14}$$

Similarly, the communication delay between the MEC device and the cloud server C can be calculated as follows:

$$W_c = \phi \frac{D}{r} \times \frac{1-P}{1+P}. \tag{15}$$

The overall structure of the obtained controller is shown in Figure 2. It searches according to the address output by the MMU and returns the corresponding result if it hits; otherwise, it sends a request to the outside to interface with the BIU.

3. Experiments

3.1. Subjects and Data Sources. In order to prove the effectiveness of the proposed volleyball player arm trajectory optimization recognition method based on chaos theory, this paper builds an experimental platform for volleyball player arm trajectory recognition through related experiments and MATLAB environment. The experimental data comes from the record of the 2017~2019 Chinese Women's Volleyball League. The game uses a French-made camera with an internal time scale of G · V16 mm and shoots two different swings of the swinging arm at position 2 from the front side. The shooting frequency is 90 frames per second. The upper edge of the reference body is 2.4 m above the ground, the height of the camera's main optical axis from the ground is 1.67 m, and the take-off point of the athlete's spike is 20 m. A total of 60 spiking moves of 5 main players were shot, and a better image frame of each spiking action was selected as experimental data.

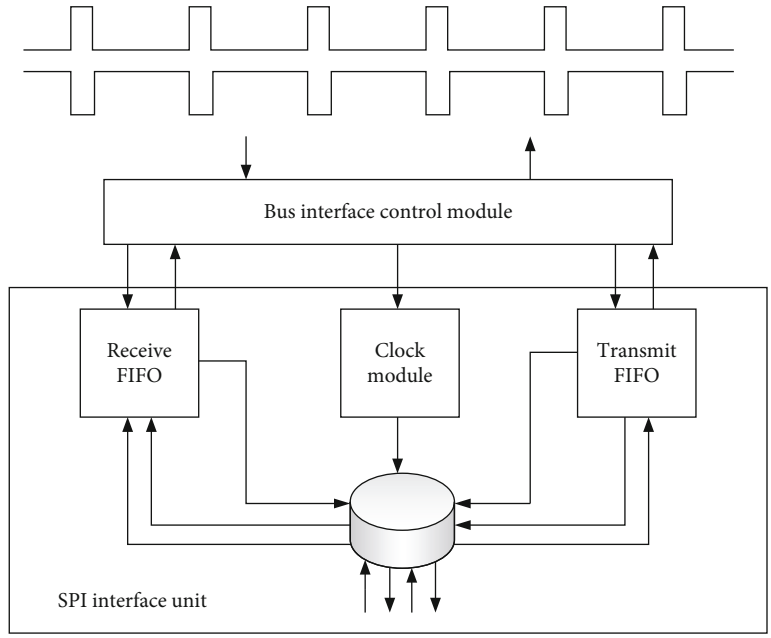

Figure 2: SPI overall structure diagram.

3.2. Experimental Software System Platform. In order to facilitate the user's operation, a software application platform with a simple graphical interface was written. The experimental platform mainly includes the following modules: data acquisition and processing module, trajectory generation module, 3D simulation module, and robot communication module, as shown in Figure 3.

This platform is modular, portable, and extensible, and at the same time, supports TCP/UDP network communication and the storage of related data and control instructions. The process flow for the robot control software to plan the robot's dynamic motion is shown in Figure 4.

The programming languages of the software platform are mainly MATLAB and C #. In order to take advantage of MATLAB's excellent numerical computing power, the processing of arm motion data, the generation of trajectories, and the three-dimensional simulation are carried out in MATLAB. The three-dimensional simulation interface establishes a three-dimensional model of the robot.

4. Discussion

4.1. Centrifugal/Centripetal Ratio Analysis. The relationship between the eccentric and centripetal ratio of the shoulder joint flexor and extensor is the relationship between the active muscle and the antagonist muscle. On the contrary, when the extensors of the shoulders perform centripetal movements, the flexors of the shoulders adjust the movement of the shoulder joints by eccentric movements. The ratio of shoulder joint antagonistic eccentric/active muscle centripetal contraction is shown in Table 2.

It is generally believed that isotonic eccentric contraction is when the tension on the tendon reaches a certain level and may damage the muscle. The Golgi tendon in the skeletal muscle tendon sends out a return impulse to the central nervous system, which has an inhibitory effect on the motor nerve. Inhibition of muscle activity can prevent muscle strain. We analyze the number of technical actions assisted by running, the distance of each step, and the distance of approach, as shown in Table 3:

The purpose of the run-up is to increase the take-off height on the one hand, and on the other hand, to obtain a certain forward momentum after the take-off, and to choose a suitable hitting point.

Combining the data in Table 2, an analysis of the shoulder joint antagonistic muscle centrifugation/active muscle centripetal ratio can be obtained, as shown in Figure 5.

During the volleyball swing arm spiking process, the flexor, abductor, and external rotation muscle groups mainly increase the angle of the shoulder joint to generate potential energy, and the extensor, internal rotation, and horizontal adduction muscle groups during the arm swing stage contract to produce strength and accelerate the movement of the upper limbs, and the flexor, external rotation, and horizontal abduction muscle groups do eccentric contraction. On the one hand, they must resist the force generated by the concentric contraction of the internal rotation muscle group. On the other hand, they must also cushion the inertia of the upper limbs to prevent the shoulder joint from concentric contraction of the internal rotator from the extreme movement beyond the physiological range in a certain direction. By regularly performing constant-speed strength test on the shoulder joint, the balance of the antagonistic eccentric eccentric force of the two shoulder joints and the centripetal force of the original motor muscle is compared to prevent the occurrence of sports injuries. The ratio of the external rotation centrifugal/internal rotation centripetal and horizontal adduction centrifugation/horizontal abduction centripetal right hand is smaller than the left hand. This discovery should attract enough attention, because the

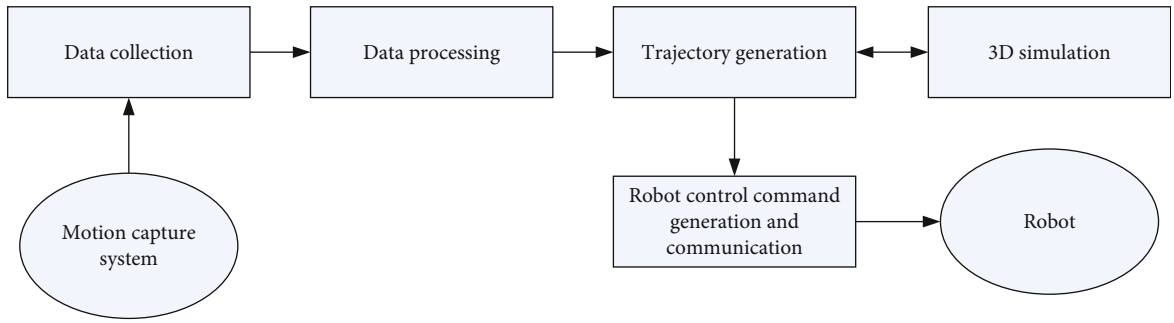

Figure 3: Software platform structure.

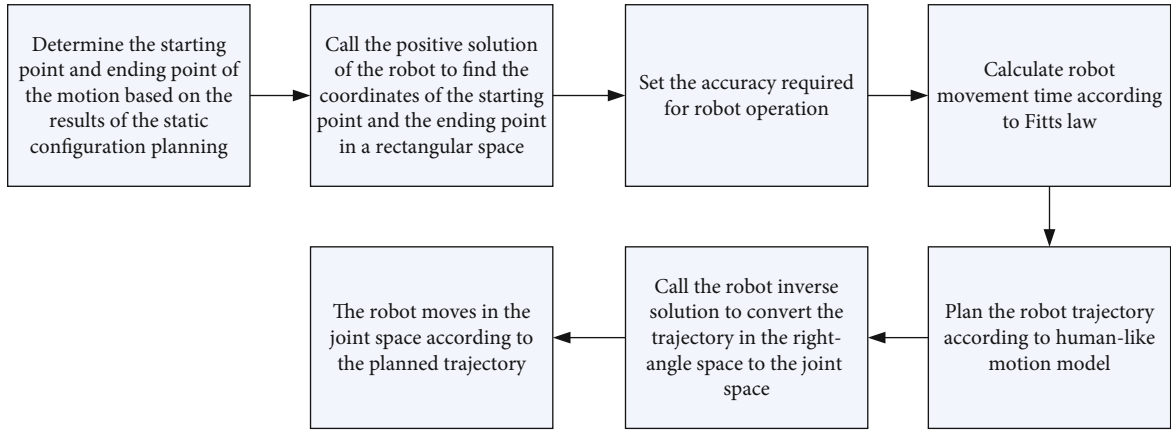

Figure 4: Robot control software to plan the processing flow of robot dynamic motion.

Table 2: Shoulder joint antagonist eccentric/active muscle centripetal contraction ratio.

Researcher	Object	Speed	Result
Yu He	Men's volleyball	60°/s	Flexion/centrifugation
Noffal	Men's baseball	60°/s	External spin centrifuge/internal spin centrifuge
Sirota	Men's tennis	60°/s	External spin centrifuge/internal spin centrifuge
Mikesky	Man athlete	60°/s	External spin centrifuge/internal spin centrifuge

Table 3: Step distances of different technologies.

	Jump serve		Back smash		Front row smash	
	L jump 1	L jump 2	L after 1	L after 2	L front 1	L front 2
1	0.75	1.01	0.74	1.04	0.64	1.30
2	0.84	1.29	0.88	1.22	1.01	0.88
3	0.78	1.05	0.91	1.14	0.86	1.11
4	0.96	1.06	1.04	1.14	1.26	0.82
5	0.72	1.03	0.88	1.18	0.76	1.17

horizontal adduction muscles and external rotation muscles play an important buffering role in the completion of the pull arm and batting movements. During the deceleration of the batting action, the centrifugal contraction of the external rotation muscle generates greater tension to control the degree of centripetal contraction of the internal rotation muscle. After frequent practice of the above movements, the overloaded work due to eccentric contraction increases the risk of muscle injury or worsening strain. Therefore, the external rotation centrifugal force and horizontal adduction centrifugal force should be strengthened to maintain the balance of shoulder joint muscle strength.

4.2. Comparative Analysis of Volleyball Players' Upper Limb Rapid Strength Kinematics Index. The shoulder rotation angle refers to the angle formed by the line between the shoulders of the athlete and the horizontal plane and represents the rotation angle of the upper body. When the tested athletes completed the entire batting action in the air, the angle change of the shoulder rotation angle at the maximum of the arm and the moment of the shot can reflect the rotation amplitude.

By analyzing the data in Table 4, it can be seen that when the male athlete has the largest arm before and after the experiment, the shoulder rotation angle differs by about 5

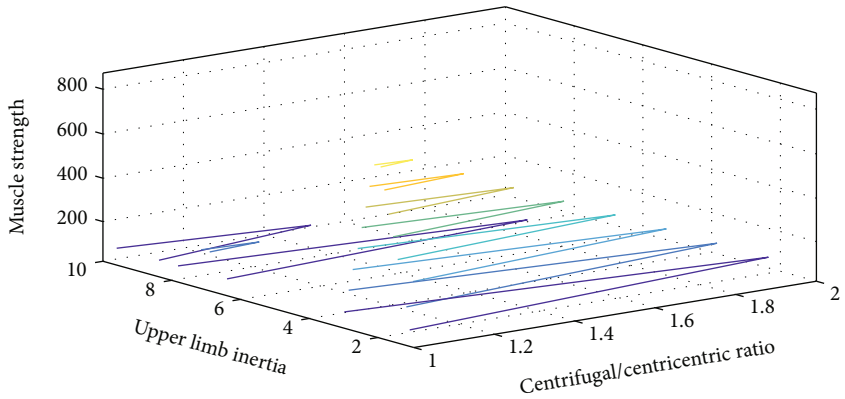

Figure 5: Analysis of the ratio of antagonistic eccentric/active muscle centripetal of the shoulder joint.

Table 4: The angle of shoulder rotation angle before and after the experiment.

		Before the experiment		After the experiment			
Gender	Batting action	Average value	Standard deviation	Average value	Standard deviation	T value	P value
Male	When the arm is maximum	42.13	2.16	47.27	2.33	0.288	<0.05
	Hitting moment	13.48	1.43	14.76	1.53	0.167	>0.05
	Angle change value	28.65	1.66	32.48	1.75	0.604	<0.05
Female	When the arm is maximum	37.62	1.87	40.12	2.06	0.316	<0.05
	Hitting moment	17.93	1.52	18.05	1.23	0.342	>0.05
	Angle change value	19.65	1.79	22.08	1.55	0.931	<0.05

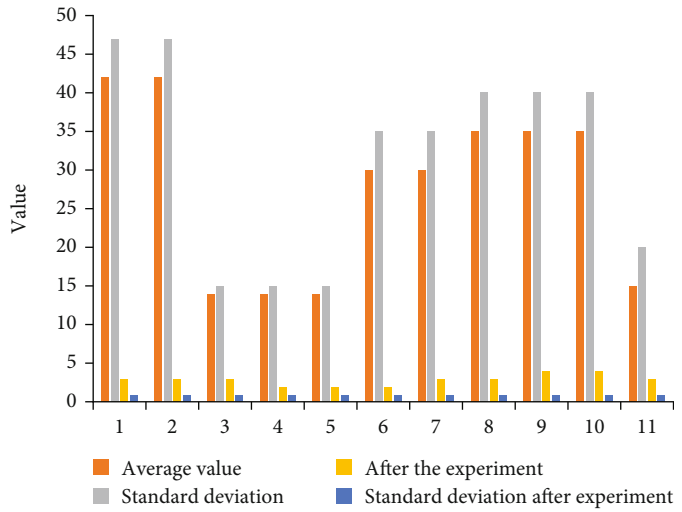

Figure 6: Comparative analysis of volleyball players' upper limb rapid strength kinematics index.

degrees, $P < 0.05$, showing a significant difference, which can be seen after the experiment. The body width has been significantly improved. Combining the data in Table 3, a comparative analysis of the volleyball players' upper limb fast strength kinematics indicators can be obtained, as shown in Figure 6.

The angle of the shoulder spin angle of the male athlete at the moment of hitting the ball did not change much, $P > 0.05$, and there was no significant difference, so the athlete did not change significantly after the experiment. The angle change value differs by about 5 degrees before and after the experiment, $P < 0.05$, showing a significant difference. It

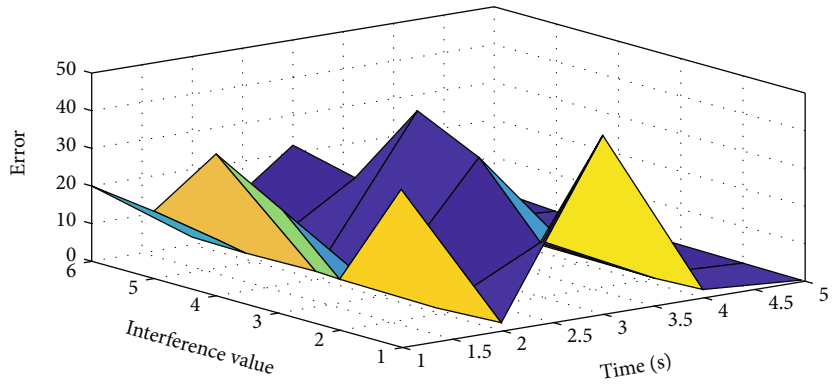

Figure 7: Actual and observed values of nonlinear disturbance observers with sliding mode adaptive inversion control.

Table 5: Take-off level analysis.

	Jump serve	Back smash	Front row smash
V and	3.02 ± 0.49	3.58 ± 0.17	3.42 ± 0.21
V double 1 (m/s)	2.08 ± 0.28	2.06 ± 0.22	1.68 ± 0.35
V double 2 (m/s)	2.53 ± 0.24	2.82 ± 0.23	2.72 ± 0.33
Horizontal speed damage rate	0.29 ± 0.07	0.38 ± 0.07	0.48 ± 0.09
Horizontal speed conversion rate	2.52 ± 0.22	2.03 ± 0.47	1.61 ± 0.47
Jump height (m)	0.71 ± 0.09	0.84 ± 0.09	0.82 ± 0.11
Jump distance (m)	1.72 ± 0.29	2.16 ± 0.17	1.55 ± 0.29

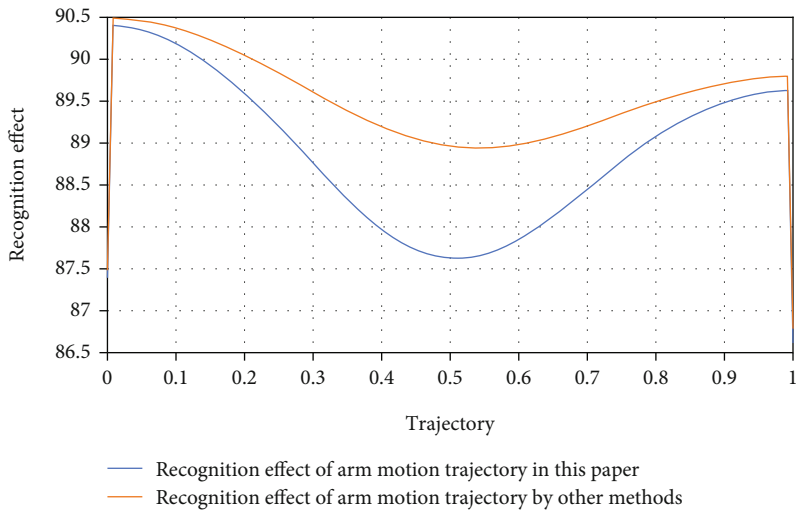

Figure 8: Comparison results of two different methods for recognizing the effect of athlete's arm trajectory.

can be seen that the amplitude of the male athlete's rotation after the experiment has increased greatly, which also shows that the athlete's spiking strength has also been compared. A large increase, the difference between the angle change value before and after the experiment is about 3 degrees, $P < 0.05$, showing a significant difference. It can be seen that the amplitude of the athlete's rotation after the experiment has increased greatly, which also shows that the athlete's spiking strength has also been greatly improved. The experimental results provide theoretical help for the optimal recognition of the volleyball player's arm movement trajectory.

4.3. Analysis of Sliding Mode Adaptive Inversion Control Based on Nonlinear Disturbance Observation. Simulation of

sliding mode adaptive inversion control based on nonlinear disturbance observation is used. Nonlinear disturbance observation is used to estimate matching interference. The purpose of the sliding mode observation period is to reduce the total interference of the system. The simulation is based on a humanoid robot and DC motor driver. The actual and observed values of the nonlinear disturbance observer for sliding mode adaptive inversion control are shown in Figure 7.

As shown in the figure, the output error of the left arm's position tracking under disturbance. It can be clearly seen that the left arm's input and position tracking error have obvious fluctuations under the interference condition. In the case of no interference, there is no fluctuation between the controller input and position tracking error between 1 and 3, the controller input is smooth and stable, and the output error is zero. Based on the above simulation analysis, it can be seen that this control method does not require the robot kinematics and dynamic model to generate any regression matrix when designing the controller. In addition, it proves that using this controller ensures that all signals of the closed-loop system converge exponentially. The tracking error consistency is ultimately bounded. The controller is suitable for performance tracking of humanoid robot arms.

The conversion rate of the horizontal speed of the back-row smash and the jump-initiated jump is much lower than that of the front-row smash. Jump serve has certain characteristics of rushing jump. The analysis of take-off level speed conversion rate is shown in Table 5:

4.4. Contrast Analysis on the Recognition Effect of Arm Motion Trajectory by Different Methods. The method of this article and other methods are used to carry out the experiment of volleyball player's arm movement trajectory recognition. Two different methods are used to compare the effect of the athlete's arm movement trajectory recognition. The comparison results are shown in Figure 8.

It can be analyzed that the effect of using this method to identify the trajectory of the arm is significantly higher than the effect of using other methods to identify the trajectory of the arm of the volleyball player. This is mainly because when using this method for arm movement trajectory recognition, it is first combined with the background difference principle to detect the athlete's movement trajectory, using color histogram particle filtering for dynamic arm tracking, and fused with chaos theory to obtain sports space. We reconstruct the athlete's arm trajectory to ensure the effectiveness of the method in this paper to identify the arm's trajectory. In the method of this paper, when the recognition of the volleyball player's arm trajectory is optimized, the phase space of the player's arm trajectory is reconstructed using chaos theory. From the reconstructed phase space, the chaotic invariant representing the trajectory of the athlete's arm is extracted, and it has three-dimensional space characteristics. The arm movement trajectory is converted into a one-dimensional arm movement trajectory. On this basis, the optimized recognition of the volleyball player's arm movement trajectory is completed, thereby ensuring the comprehensive effectiveness of the volleyball player's arm movement trajectory identification method.

5. Conclusions

In this paper, when the current method is used to identify the movement trajectory, the characteristics of the athlete's arm movement trajectory cannot be accurately extracted, and the volleyball player's arm movement trajectory cannot be accurately identified. A new method for volleyball player's arm trajectory optimization recognition based on chaos theory is proposed. The simulation results show that the proposed method has high recognition accuracy and provides a strong scientific basis for improving the volleyball player's spiking technique.

This article focuses on the research of the volleyball player's arm movement mechanism. The goal is to reproduce the human's coordinated movement of the human arm on the humanoid two-armed robot. Systematic and in-depth research has been carried out on aspects such as rotational motion evaluation, human trajectory capture and inverse kinematics, model matching between human trajectory and dual-arm robot, and coordinated control method of dual-arm.

There are still some deficiencies in this paper. Although this paper has made some research progress, it still needs to further optimize the algorithm in human motion capture, and the experimental design needs to increase the sample value. In terms of control algorithm, the control space of the dual-arm robot is still very large, and there are still many problems that need further research.

Data Availability

No data were used to support this study.

Conflicts of Interest

The authors declare that they have no conflicts of interest.

Authors' Contributions

Ming Liu contributed to the writing and editing. Jingtao Wu contributed to the formal analysis. Jiangang Tao contributed to the methodology.

References

[1] E. I. Barakova, P. Bajracharya, M. Willemsen, T. Lourens, and B. Huskens, "Long-term LEGO therapy with humanoid robot for children with ASD," *Expert Systems*, vol. 32, no. 6, pp. 698–709, 2015.

[2] W. He, W. Ge, Y. Li, Y. J. Liu, C. Yang, and C. Sun, "Model identification and control design for a humanoid robot," *IEEE Transactions on Systems Man & Cybernetics Systems*, vol. 47, no. 1, pp. 1–13, 2016.

[3] M. Fakoor, A. Kosari, and M. Jafarzadeh, "Humanoid robot path planning with fuzzy Markov decision processes," *Social Science Electronic Publishing*, vol. 14, no. 5, pp. 300–310, 2016.

[4] J. Zhao, X. Mao, H. Hu, L. Niu, and G. Chen, "Behavior-based SSVEP hierarchical architecture for telepresence control of humanoid robot to achieve full-body movement," *IEEE Transactions on Cognitive and Developmental Systems*, vol. 9, no. 2, pp. 197–209, 2017.

[5] E. Tidoni, P. Gergondet, G. Fusco, A. Kheddar, and S. M. Aglioti, "The role of audio-visual feedback in a thought-based control of a humanoid robot: a BCI study in healthy and spinal cord injured people," *IEEE Transactions on Neural Systems & Rehabilitation Engineering*, vol. 25, no. 6, pp. 772–781, 2017.

[6] J. Baltes, K. Y. Tu, S. Sadeghnejad, and J. Anderson, "Huro-Cup-competition for multi-event humanoid robot athletes," *Knowledge Engineering Review*, vol. 1, no. 1, pp. 1–14, 2016.

[7] F. Guo, T. Mei, M. Luo et al., "Motion planning for humanoid robot dynamically stepping over consecutive large obstacles," *Industrial Robot*, vol. 43, no. 2, pp. 204–220, 2016.

[8] J. Andreu-Perez, F. Cao, H. Hagras, and G. Z. Yang, "A self-adaptive online brain–machine interface of a humanoid robot through a general type-2 fuzzy inference system," *IEEE Transactions on Fuzzy Systems*, vol. 26, no. 1, pp. 101–116, 2018.

[9] S. Guo, H. Xu, N. M. Thalmann, and J. Yao, "Customization and fabrication of the appearance for humanoid robot," *The Visual Computer*, vol. 33, no. 1, pp. 63–74, 2017.

[10] F. Guo, T. Mei, M. Ceccarelli, Z. Zhao, T. Li, and J. Zhao, "A generic walking pattern generation method for humanoid robot walking on the slopes," *Industrial Robot*, vol. 43, no. 3, pp. 317–327, 2016.

[11] T. Kishi, S. Shimomura, H. Futaki et al., "Development of a humorous humanoid robot capable of quick-and-wide arm motion," *IEEE Robotics and Automation Letters*, vol. 1, no. 2, pp. 1081–1088, 2016.

[12] M. Rogóż, H. Zeng, C. Xuan, D. S. Wiersma, and P. Wasylczyk, "Soft robotics: light-driven soft robot mimics caterpillar locomotion in natural scale (advanced optical materials 11/2016)," *Optical Materials*, vol. 4, no. 11, pp. 1902–1902, 2016.

[13] C. Yang, T. Teng, B. Xu, Z. Li, J. Na, and C. Y. Su, "Global adaptive tracking control of robot manipulators using neural networks with finite-time learning convergence," *International Journal of Control Automation & Systems*, vol. 15, no. 4, pp. 1916–1924, 2017.

[14] M. Geravand, P. Z. Korondi, C. Werner, K. Hauer, and A. Peer, "Human sit-to-stand transfer modeling towards intuitive and biologically-inspired robot assistance," *Autonomous Robots*, vol. 41, no. 3, pp. 575–592, 2017.

[15] R. Caccavale and A. Finzi, "Flexible task execution and attentional regulations in human-robot interaction," *IEEE Transactions on Cognitive and Developmental Systems*, vol. 9, no. 1, pp. 68–79, 2017.

[16] B. Fang, Q. Zhang, H. Wang, and X. Yuan, "Personality driven task allocation for emotional robot team," *International Journal of Machine Learning and Cybernetics*, vol. 9, no. 12, pp. 1955–1962, 2017.

[17] C. Nomine-Criqui, A. Germain, A. Ayav, L. Bresler, and L. Brunaud, "Robot-assisted adrenalectomy: indications and drawbacks," *Updates in Surgery*, vol. 69, no. 2, pp. 127–133, 2017.

[18] M. N. V. Oosterom, H. Simon, L. Mengus et al., "Revolutionizing (robot-assisted) laparoscopic gamma tracing using a drop-in gamma probe technology," *American Journal of Nuclear Medicine and Molecular Imaging*, vol. 6, no. 1, pp. 1–17, 2016.

[19] E. Celik, R. Semrau, C. Baues, M. Trommer-Nestler, W. Baus, and S. Marnitz, "Robot-assisted extracranial stereotactic radiotherapy of adrenal metastases in oligometastatic non-small cell lung cancer," *Anticancer Research*, vol. 37, no. 9, pp. 5285–5291, 2017.

[20] D. Ao, R. Song, and J. W. Gao, "Movement performance of human-robot cooperation control based on EMG-driven Hill-type and proportional models for an ankle power-assist exoskeleton robot," *IEEE Transactions on Neural Systems & Rehabilitation Engineering*, vol. 25, no. 8, pp. 1125–1134, 2017.

[21] D. H. Lim, W. S. Kim, H. J. Kim, and C. S. Han, "Development of real-time gait phase detection system for a lower extremity exoskeleton robot," *International Journal of Precision Engineering & Manufacturing*, vol. 18, no. 5, pp. 681–687, 2017.

[22] M. E. Giannaccini, C. Xiang, and A. Atyabi, "Novel design of a soft lightweight pneumatic continuum robot arm with decoupled variable stiffness and positioning," *Soft Robotics*, vol. 5, no. 1, pp. 54–70, 2018.

[23] H. Mehdi and O. Boubaker, "PSO-Lyapunov motion/force control of robot arms with model uncertainties," *Robotica*, vol. 34, no. 3, pp. 634–651, 2016.

[24] A. Izadbakhsh and S. Khorashadizadeh, "Robust task-space control of robot manipulators using differential equations for uncertainty estimation," *Robotica*, vol. 35, no. 9, pp. 1923–1938, 2017.

[25] Y. Shi, Y. Tian, Y. Wang, and T. Huang, "Sequential deep trajectory descriptor for action recognition with three-stream CNN," *IEEE Transactions on Multimedia*, vol. 19, no. 7, pp. 1510–1520, 2017.

[26] C. S. Fahn, C. Y. Kao, C. B. Yao, and M. L. Wu, "Exploiting AdaRank model and trajectory of hand motion for hand gesture recognition," *Sensor Letters*, vol. 14, no. 10, pp. 1061–1065, 2016.

[27] L. Zhou, S. Bai, and Y. Li, "Energy optimal trajectories in human arm motion aiming for assistive robots," *Modeling, Identification and Control (MIC)*, vol. 38, no. 1, pp. 11–19, 2017.